

# Effects of Postweld Aging Treatment on Rotary Bending Fatigue Strength of Friction Welded Joints at Elevated Temperature

Sae Kyoo Oh, Sang Deok Han and Uh Joh Lim

마찰 용접부의 고온 회전굽힘 피로 강도에 미치는 용접후 시효열처리의 영향에 관한 연구

오세규\* · 한상덕\* · 임우조\*

## 요 약

최근 높은 경제성과 용접성의 우수성에 의한 마찰 용접의 응용에 있어서 내열·내식 재료가 개스터어핀, 기관, 핵 발전기등의 기계 부품 생산 공업에 널리 이용되고 있다. 따라서 이중내열 합금강의 마찰 용접된 부품을 이용함에 있어서 내식·내마모 및 용접성 뿐만 아니라 고온 피로 강도와 크리이프 강도 등의 복합 특성에 관한 연구가 요구되고 있다.

본 연구에서는 마르텐사이트계 실크롬 내열강과 오오스테나이트계 니켈크롬 스테인레스강의 이중 내식·내열 합금강이 최적 용접조건하에서 마찰 용접된 후의 시효 열처리가 용접재의 700°C 고온 회전 굽힘 피로강도 특성에 미치는 영향에 관하여 실험과 강도해석에 의해 조사되었고 용접후의 용체화 처리와 시효 열처리법에 의한 내열강 마찰 용접강도 개선법을 개발코자한 것이다.

## 1. Introduction

Nowadays, in friction welding application for both economical and technical advantages, heat-resisting and anticorrosive materials are widely used in the industrial production fields of the mechanical components such as those of gas turbines, engines, nuclear power plants, etc. It is because, for example, the friction-welded exhaust valve of internal combustion engine should be operated under mechanical-repeating load in the environment of high-pressured-exp-

loded gas at the elevated temperature of about 700 through 800°C. Thus the composite special properties such as high temperature fatigue strength and creep strength as well as anti-corrosiveness, anti-abrasion and weldability are particularly and simultaneously required for in utilizing those friction-welded components of heat-resisting dissimilar alloys.

Recently, there have been many reports<sup>1,2)</sup> on the high temperature fatigue strength<sup>3,4)</sup> on those of friction welded joints especially as aging treated<sup>5)</sup>, in the case of which

---

\* Member, Dept. of Mechanical Engineering, Faculty of Engineering, National Fisheries University of Busan, Busan, Korea.

the nickel base alloys (Udimet 700) were friction-welded and age-treated for creep tests.

In this study, the dissimilar alloys of Si-Cr base heat resisting steels SUH3 and Ni-Cr base stainless steels SUS303 were friction-welded under the proper welding

conditions, and then the effects of postweld aging treatment on the high temperature (700°C) rotary bending fatigue strength of those welded joints were investigated for the purpose of improving the weld strength by postweld aging treatment after postweld solution treatment<sup>6)</sup>.

**Table 1. Chemical compositions of materials (wt %).**

Materials	C	Si	Mn	P	S	Cr	Mo	Ni
SUH3	0.43	2.20	0.33	0.027	0.009	12.26	0.87	—
SUS303	0.06	0.49	1.56	0.026	0.296	17.65	—	8.55

**Table 2. Mechanical properties of materials.**

Materials	Tensile strength $\sigma_T$ (kgf/mm <sup>2</sup> )	Yield strength $\sigma_Y$ (kgf/mm <sup>2</sup> )	Elongation $\epsilon$ (%)	Hardness Hv
SUH3	102.0	70.0	15.0	254
SUS303	63.3	26.3	59.3	206

## 2. Specimens and Experimental Procedures

The materials of specimens used are the heat-resisting and corrosion-resisting steels such as the wrought stainless martensitic sil-chromium steels SUH3 and the austenitic nickel-chromium stainless steels SUS303, both of which are domestic-made. Their chemical compositions and mechanical properties are listed in Table 1 and Table 2, respectively.

Figure 1 shows the dimensions and configurations of welding workpieces for friction welding, tension test specimen and rotary bending fatigue test specimens for both base metal and welded joint. Each pair of workpieces faced on the mating ends was welded on the continuous drive friction welding machine (Toshiba FW-30) under the pre-determined proper welding conditions as listed in Table 3.

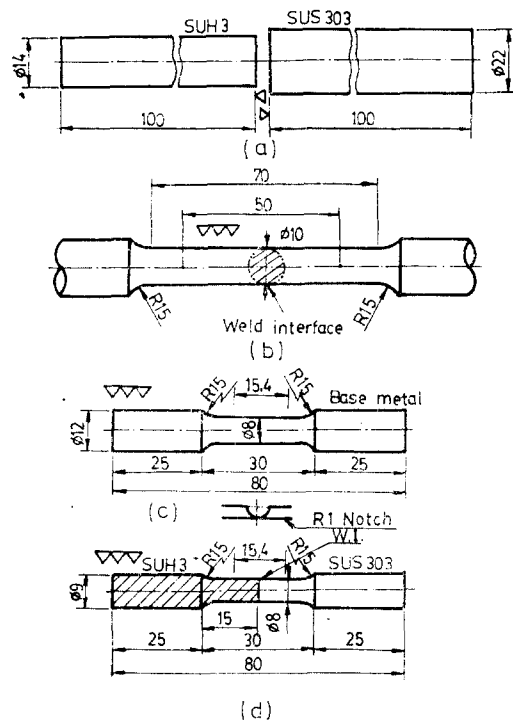


**Fig. 1.** Dimensions and configurations of specimens. (a) Welding workpiece, (b) Tension test specimen, (c), (d) Rotary bending fatigue test specimen with notch.

After welding, all the flashes were eliminated by turning or grinding, and the specimens for tension and rotary bending fatigue tests were machined and ground as shown in Figure 1.

And then a part of those specimens were heat-treated at the conditions such as the solution treatment of one hour at 1060°C and water cooling (14°C) and soon the aging treatment of 10 and 100 hours at

700°C and air cooling at room temperature to investigate the aging effects on fatigue properties of both base metals and welded joints at the elevated temperature of 700°C. The heating furnace was an electric muffle furnace (Shimadzu Model SMF-14). The mechanical properties of base metals SUH3 and SUS303 heat-treated as above mentioned are shown in Table 4.

Table 3. Welding conditions.

Materials to be welded	Rotating speed $n$ (rpm)	Heating pressure $P_1$ (kgf·mm <sup>-2</sup> )	Upsetting pressure $P_2$ (kgf·mm <sup>-2</sup> )	Total upset $u$ (mm)	Heating time $t_1$ (s)	Upsetting time $t_2$ (s)
SUH3 to SUS303	2420	8	22	7	3	2

Table 4. Mechanical properties according to heat treatment.

Materials	Heat treatment	Tensile strength $\sigma_T$ (kgf·mm <sup>-2</sup> )	Yield strength $\sigma_Y$ (kgf·mm <sup>-2</sup> )	Elongation (%)	Hardness Hv
SUH3	Solution treat.* (0 h aging)	124.7	80.0	13.8	300
	10 h aging**	94.0	69.7	19.4	262
	100 h aging**	86.8	34.3	12.6	252
SUS303	Solution treat. (10 h aging)	66.9	28.1	59.6	211
	10 h aging	71.1	25.6	53.6	206
	100 h aging	55.3	19.0	53.2	218

\* 1060°C×1 h, 14°C water cooling

\*\* 700°C×10 h (or 100 h), air cooling, just after solution treatment.

After heat treatment, the parallel parts of the specimens were polished with emery papers of #01 through #04 and buffed with chromium oxide to avoid the surface roughness effect during test.

For the fatigue tests at the elevated temperature of 700°C, the Ono's high temperature rotary bending fatigue testing machine (Shimadzu Model H5, capacity 10 kgfm, 3400 cpm) was used. When the fatigue test specimen reached the temperature of 700°C in the furnace, the load was made to be

acted at the constant temperature of 700°C until the fracture occurred. For obtaining the fatigue limits and the S-N equations and curves, the method using the Pantereb's equation<sup>7-9)</sup> was taken.

For microscopical examination, the composition of HNO<sub>3</sub> 10cc, HCl 20cc and glycerol 10cc was used as an etching reagent, while the composition rate 2:7 of HClO<sub>4</sub> and CH<sub>3</sub>COOH including Al of about 0.5 % was used as an electrolytic polishing reagent.

Table 5. Comparison of fatigue strength between the Pantereb's calculated and the empirical values.

Specimens for rotary bending fatigue test	S-N curves	Number of cycles		Rotary bending stress(kgf/mm <sup>2</sup> )		Fatigue limit (kgf/mm <sup>2</sup> )		
		N <sub>1</sub>	N <sub>2</sub>	σ <sub>1</sub>	σ <sub>2</sub>	calculated σ <sub>FC</sub>	empirical σ <sub>FE</sub>	% difference of σ <sub>FE</sub> from σ <sub>FC</sub>
SUH3 (R. T.)	S3	1.15×10 <sup>4</sup>	2.361×10 <sup>5</sup>	56.85	51.49	51.17	49.56	
SUH3 with 1mmR notch (R. T.)	S3n	5.99×10 <sup>4</sup>	2.352×10 <sup>5</sup>	28.38	23.30	22.27	20.86	
SUH3(700°C specimen)	S3T	2.35×10 <sup>4</sup>	6.020×10 <sup>5</sup>	17.46	11.50	11.37	11.01	
SUH3 as solution treated*(700°C specimen)	S <sub>700A</sub>	3.84×10 <sup>4</sup>	3.158×10 <sup>5</sup>	26.25	18.19	17.56	17.06	
SUH3 as 10 h aging treated**(700°C specimen)	S <sub>700A</sub>	1.61×10 <sup>4</sup>	1.359×10 <sup>5</sup>	26.55	23.19	22.83	19.31	
SUH3 as 100 h aging treated**(700°C specimen)	S <sub>700A</sub>	1.02×10 <sup>4</sup>	4.483×10 <sup>5</sup>	25.12	20.07	19.99	18.05	
SUS303 (R. T.)	S303	5.07×10 <sup>4</sup>	4.651×10 <sup>5</sup>	37.11	31.84	31.27	27.83	
SUS303 with 1mmR notch (R. T.)	S303n	7.14×10 <sup>4</sup>	4.128×10 <sup>5</sup>	24.43	18.97	18.23	17.71	
SUS303 (700°C specimen)	S303T	1.86×10 <sup>4</sup>	7.020×10 <sup>5</sup>	10.45	10.02	10.01	10.01	mean(%)
SUS303 as solution treated*(700°C specimen)	S303T <sub>100A</sub>	2.36×10 <sup>4</sup>	1.272×10 <sup>5</sup>	16.84	14.73	14.05	11.80	-7.5
SUS303 as 10h aging treated**(700°C specimen)	S303T <sub>100A</sub>	1.21×10 <sup>4</sup>	5.990×10 <sup>4</sup>	15.92	14.48	14.17	12.87	
SUS303 as 100 h aging treated**(700°C specimen)	S303T <sub>100A</sub>	2.58×10 <sup>4</sup>	3.350×10 <sup>4</sup>	15.61	15.38	14.68	13.06	
F. W. J. (SUH3-SUS303)	W	1.41×10 <sup>4</sup>	2.281×10 <sup>5</sup>	27.89	25.12	24.97	24.06	
F. W. J. (SUH3-SUS303) (700°C specimen)	W <sub>T</sub>	1.12×10 <sup>4</sup>	2.250×10 <sup>5</sup>	14.05	11.50	11.40	11.00	
F. W. J. as solution treated*(700°C specimen)	W <sub>700A</sub>	1.91×10 <sup>4</sup>	1.665×10 <sup>5</sup>	17.06	14.78	14.55	12.07	
F. W. J. as 10 h aging treated**(700°C specimen)	W <sub>700A</sub>	2.41×10 <sup>4</sup>	1.248×10 <sup>5</sup>	18.19	17.01	16.76	15.87	
F. W. J. as 100h aging treated**(700°C specimen)	W <sub>700A</sub>	1.99×10 <sup>4</sup>	6.010×10 <sup>4</sup>	18.10	17.79	16.00	15.03	

\* Solution treatment; 1060°C×1 h, 14°C water cooling

\*\* Aging treatment; 700°C×10 h (or 100 h), air cooling, just after solution treatment.

### 3. Results and Discussions

#### 3-1. S-N Diagrams and Empirical Equations

The rotary bending fatigue tests were carried out at the room temperature and the elevated temperature of 700°C in order to investigate the fatigue strength properties of the dissimilar heat resisting steels friction-welded joints (SUH3-SUS303) welded under the proper welding conditions as in Table 3 and heat treated as in Table 4 and Table 5. Every calculated fatigue limit ( $\sigma_{FC}$ ) obtained from each two experimental points by Pantereb's equation<sup>7)</sup>

$$\sigma_{FC} = \sqrt{\frac{(N_2 - N_1)\sigma_1^2\sigma_2^2}{N_2\sigma_1^2 - N_1\sigma_2^2}} \dots\dots\dots(1)$$

was compared with every empirical fatigue limit ( $\sigma_{FE}$ ) as shown in Table 5. The values of  $\sigma_{FC}$  and  $\sigma_{FE}$  are also almost same and the mean difference is -7.5%, namely,

$\sigma_{FC}$  is only about 1.42 kg/mm<sup>2</sup> higher than  $\sigma_{FE}$  in mean.

Every calculated fatigue limit including S-N curves and every empirical S-N curve computed from all the data points by the least squares method are shown in Figure 2, Figure 3 and Figure 4. Those computed empirical equations are as follows:

$$S_3 \quad ; \log N = 6.4297 - (0.7135\sigma_B - 35.1897)^{0.5}, (\sigma_B \geq 49.56) \dots\dots\dots(2)$$

$$S_{3n} \quad ; \log N = 6.4445 - (0.3629\sigma_B - 7.4633)^{0.5}, (\sigma_B \geq 20.86) \dots\dots\dots(3)$$

$$S_{3T} \quad ; \log N = 6.8421 - (0.8772\sigma_B - 9.1593)^{0.5}, (\sigma_B \geq 11.01) \dots\dots\dots(4)$$

$$S_{3T0A} \quad ; \log N = 5.9639 - (0.2511\sigma_B - 4.2837)^{0.5}, (\sigma_B \geq 17.06) \dots\dots\dots(5)$$

$$S_{3T10A} \quad ; \log N = 10.8901 - (3.5522\sigma_B - 46.9105)^{0.5}, (\sigma_B \geq 19.31) \dots\dots\dots(6)$$

$$S_{3T100A} \quad ; \log N = 7.7615 - (1.9321\sigma_B - 33.7735)^{0.5}, (\sigma_B \geq 18.05) \dots\dots\dots(7)$$

$$S_{303} \quad ; \log N = 6.8211 - (0.5285\sigma_B - 15.0457)^{0.5}, (\sigma_B \geq 28.47) \dots\dots\dots(8)$$

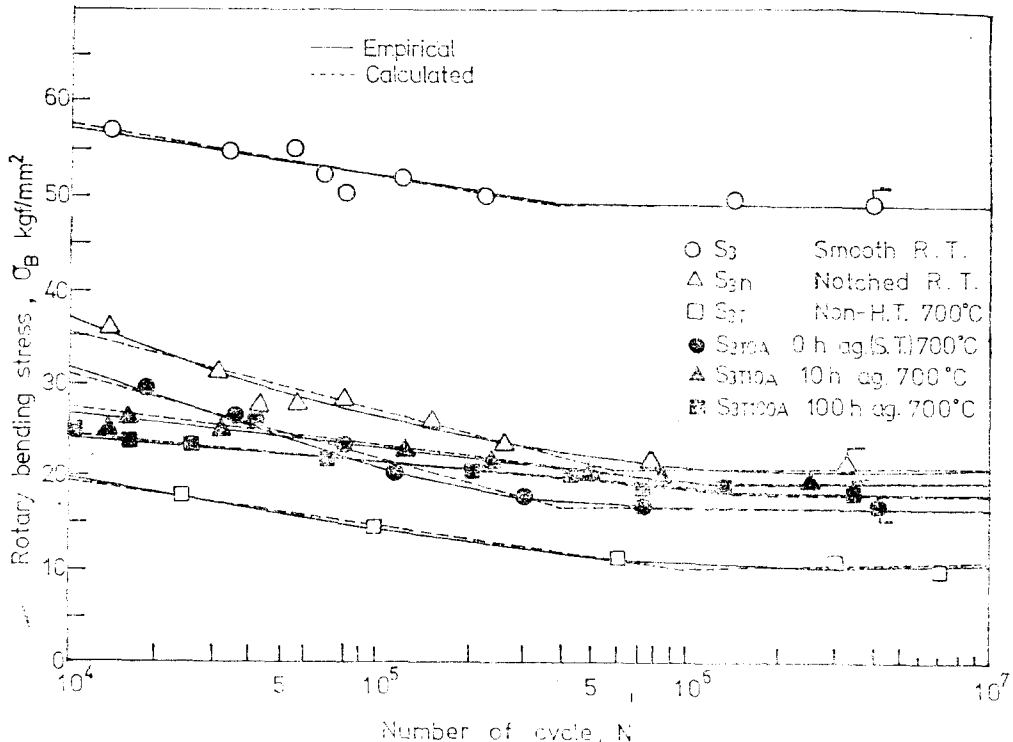


Fig. 2. S-N curves of base metal SUH3.

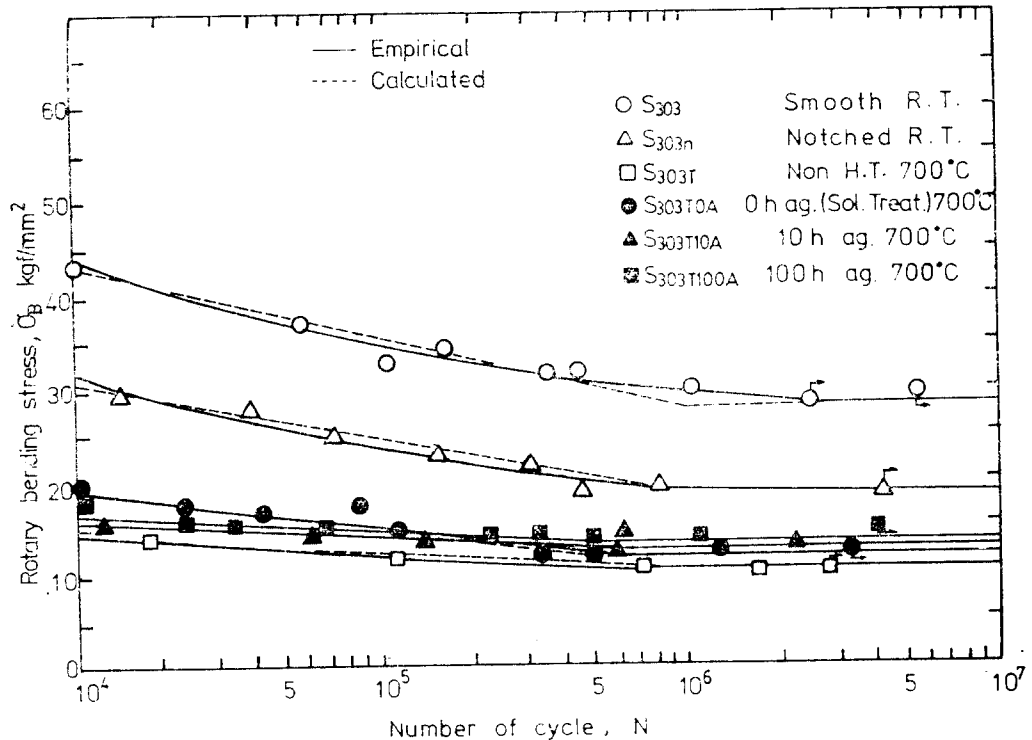


Fig. 3. S-N curves of base metal SUS303.

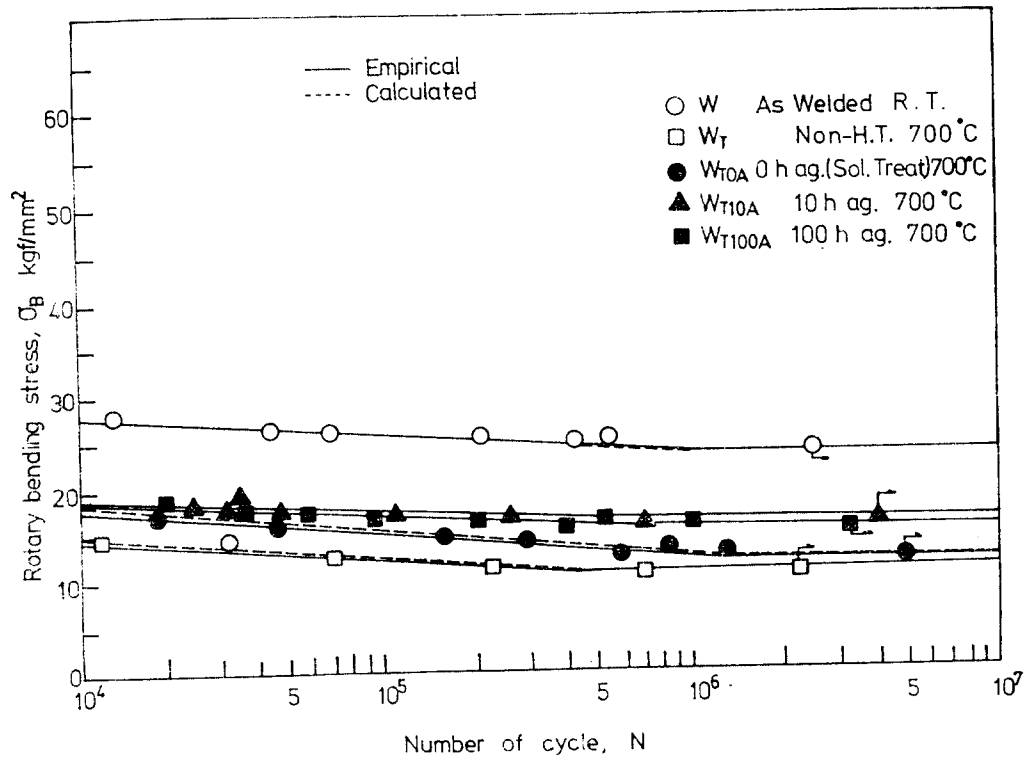


Fig. 4. S-N curves of friction welded joint SUH3-SUS303.

$$S303n; \log N = 7.0694 - (0.6232\sigma_B - 10.4763)^{0.5}, (\sigma_B \geq 17.71) \dots \dots (9)$$

$$S303T; \log N = 20.0000 - (100.0000\sigma_B - 789.0000)^{0.5}, (\sigma_B \geq 10.01) \dots \dots (10)$$

$$S303_{T0A}; \log N = 8.0540 - (1.8568\sigma_B - 19.1058)^{0.5}, (\sigma_B \geq 11.80) \dots \dots (11)$$

$$S303_{T10A}; \log N = 8.5510 - (5.4362\sigma_B - 66.7375)^{0.5}, (\sigma_B \geq 12.87) \dots \dots (12)$$

$$S303_{T100A}; \log N = 7.3500 - (2.7250\sigma_B - 33.9424)^{0.5}, (\sigma_B \geq 13.06) \dots \dots (13)$$

$$W; \log N = 6.9262 - (1.8057\sigma_B - 42.5854)^{0.5}, (\sigma_B \geq 24.06) \dots \dots (14)$$

$$W_T; \log N = 6.5094 - (1.8868\sigma_B - 20.6084)^{0.5}, (\sigma_B \geq 11.00) \dots \dots (15)$$

$$W_{T0A}; \log N = 8.2457 - (3.0473\sigma_B - 34.2933)^{0.5}, (\sigma_B \geq 12.07) \dots \dots (16)$$

$$W_{T10A}; \log N = 9.5961 - (8.7566\sigma_B - 130.4816)^{0.5}, (\sigma_B \geq 15.87) \dots \dots (17)$$

$$W_{T100A}; \log N = 8.0382 - (4.2247\sigma_B - 61.8575)^{0.5}, (\sigma_B \geq 15.03) \dots \dots (18)$$

The adequacy test result by error analysis for the above S-N empirical equations reveals that the mean of the total % errors is only 1.30% while 1.80% by Weibull's method<sup>10,11)</sup> and 2.96% by Stüssi's<sup>12)</sup>. This result suggests that the above empirical S-N equations have also a high confidence as shown in the preceding report<sup>8,9)</sup> and also can be modeled as the following;

$$\log N = -(a\sigma_B + b)^{0.5} + c \dots \dots (19)$$

where a, b, c are constants concerning materials, welding conditions or both. ☐

**3-2. Fatigue Strength and Fatigue Limit**

Comparing with both fatigue strength and fatigue limit of S-N curves S3, S3n and S3T for the base metal SUH3 in the preceding report<sup>9)</sup> those of S-N curves S3 and S3n in Figure 2 (or Equations (2) and (3), respectively) are about 13.9% lower in

mean for the fatigue strength and 8.0% lower for the fatigue limit at the room temperature fatigue test, but almost the same at the elevated temperature (700°C); This seems due to the very small amount of the chemical compositions difference such as the increase of C 0.01%, Cr 0.96% and Mo 0.14% while the decrease of Si 0.02% in the latter case, in which the fatigue notch factor ( $\beta$ ) and notch sensitivity factor ( $\eta$ ) are increased 7.7% and 13.9% more, respectively, resulting in a sudden decrease of the fatigue strength and limit from S3 to S3n as shown in Figure 2, Figure 7, Figure 8 or Table 6.

In Figure 2, Figure 3 and Figure 4, or by Equations (2) through (18), the magnitude of all the fatigue strengths ( $\sigma_B$ ) at  $N=10^4$  and  $N=10^5$  cycles and the fatigue limits ( $\sigma_F$  or  $\sigma_{FE}$ ) is;

- $\sigma_B$  at  $N=10^4$ ;  $S3 > S303 > S3n > S3_{T0A} > S303n > W > S3_{T10A} > S3_{T100A} > S3_T > S303_{T0A} > W_{T10A} \doteq W_{T100A} > W_{T0A} > S303_{T100A} > S303_{T10A} > W_T > S303_T$ ,
- $\sigma_B$  at  $N=10^5$ ;  $S3 > S303 > S3n > W > S303n > S3_{T10A} > S3_{T100A} > S3_{T0A} > W_{T10A} > W_{T100A} > S303_{T0A} > W_{T0A} > S303_{T10A} > S303_{T100A} > S3_T > W_T > S303_T$ ,
- $\sigma_{FE}$  (or  $\sigma_F$ );  $S3 > S303 > W > S3n > S3_{T10A} > S3_{T100A} > S303n > S3_{T0A} > W_{T10A} > W_{T100A} > S303_{T100A} > S303_{T10A} > W_{T0A} > S303_{T0A} > S3_T > W_T > S303_T$ .

From the above magnitude and the figures, especially it is confirmed that both high temperature (700°C) fatigue strengths  $\sigma_B$  at  $N=10^4$  and  $N=10^5$  and fatigue limit  $\sigma_{FE}$  (or  $\sigma_F$ ) of the welded joint SUH3-SUS303 ( $W_{T10A}$ ) as 10 hour aging treated were increased about 29.6%, 42.7% and

44.3% more, respectively than those of the non-heat-treated (or as welded joint ( $W_T$ )). And, in view of the postweld heat treatment effect on the high temperature fatigue limit, by solution treatment (0 hour aging), 10 hour aging or 100 hour aging-treatment, that of the welded joint was increased 9.73%, 44.27% or 36.34% more, respectively, than that of such non-heat-treated joint, too, while 17.88%, 28.57% or 30.47% more in the case of base metal SUH3 and 17.88%, 28.57% or 30.47% more, respectively, in the case of base metal SUS303. And the high temperature fatigue strengths and fatigue limit of base metal SUS303 ( $S303_T$ ) was the lowest, resulting in the high temperature fatigue fracture occurring at the base metal SUS303 side.

In the meantime, the room-temperature fatigue fracture took place at the SUS303 side ( $S303$  or  $S303_n$ ) HAZ of the welded joint ( $W$ ) due to such decrease of its room temperature fatigue strengths ( $\sigma_B$  at  $N=10^4$  and  $N=10^5$ ) and fatigue limit ( $\sigma_F$ ) as about 34.9%, 26.2% and 13.5%, respectively, from those of base metal SUS303.

Consequently, it was clarified that the high temperature fatigue strength of the friction welded joint can be increased by postweld aging treatment and have seemingly a dependence upon aging time.

### 3-3. Fatigue Life Factor

As shown in Table 6, the fatigue life factors ( $K$ ) of both the base metals ( $S3_{T0A}$ ,  $S303_{T0A}$ ) and the welded joint ( $W_{T0A}$ ) at the high temperature rotary bending fatigue

Table 6. Fatigue life factor  $K$  and fatigue life  $N_F$ .

Specimens	$\beta$	$\eta$	$K$	$N_F$ , cycles	$\sigma_F$ , kgf/mm <sup>2</sup>
S3	—	—	6.31	$3.4 \times 10^5$	49.56
S3n	2.38	1.97	4.01	$5.8 \times 10^5$	20.86
S3 <sub>T</sub>	—	—	7.12	$9.0 \times 10^5$	11.01
S3 <sub>T0A</sub>	—	—	3.73	$4.9 \times 10^5$	17.06
S3 <sub>T10A</sub>	—	—	8.14	$1.0 \times 10^6$	19.31
S3 <sub>T100A</sub>	—	—	11.43	$1.3 \times 10^6$	18.05
S303	—	—	4.17	$9.4 \times 10^5$	27.83
S303n	1.57	0.87	5.40	$8.0 \times 10^5$	17.71
S303 <sub>T</sub>	—	—	14.30	$8.5 \times 10^5$	10.01
S303 <sub>T0A</sub>	—	—	7.12	$5.0 \times 10^5$	11.80
S303 <sub>T10A</sub>	—	—	16.34	$6.1 \times 10^5$	12.87
S303 <sub>T100A</sub>	—	—	14.30	$6.9 \times 10^5$	13.06
W	—	—	14.30	$1.0 \times 10^6$	24.06
W <sub>T</sub>	—	—	12.71	$4.2 \times 10^5$	11.00
W <sub>T0A</sub>	—	—	11.43	$1.1 \times 10^6$	12.07
W <sub>T10A</sub>	—	—	19.08	$7.0 \times 10^5$	15.87
W <sub>T100A</sub>	—	—	16.35	$6.0 \times 10^5$	15.03

$\beta$ : fatigue notch factor,  $\eta$ : notch sensitivity factor,  $N_F$ : fatigue life,  $\sigma_F$ : fatigue limit.



test are decreased as much as 47.6%, 50.2% and 10.0%, respectively, from those of the non-heat treated ones as solution treated (by rapid cooling after maintaining 1060°C for 1 hour), resulting in the steeper slope of the S-N curves, decreasing normally the fatigue life. However, by 10 hour aging treatment, they were increased 14.3%, 14.3% and 50.1% more, respectively, resulting in the possibility of the fatigue life increase. Meanwhile, by 100 hour aging treatment, they were also increased 60.5%, 0% and 28.2% more, respectively, but not much significant in the case of the base metal SUS303 and the welded joint.

It seems that the cause of such steeper slope tendency<sup>13)</sup> of S-N curves by the decrease of fatigue life factor through such solution treatment could be explained as the following; though the tensile strength and hardness could be improved higher by the solution treatment of rapid cooling after maintaining 1060°C for 1 hour (Table 4), such super-saturated solid solution in the material would be put into the high temperature of 700°C during rotary bending fatigue test, and then the precipitation nuclei formation and growth and the mid-phase<sup>14)</sup> precipitation for an equilibrium phase under the unstable condition would be progressed at the early stage but, at the same time, affected by the high speed repeating tension-compression stress during the rotary bending test, resulting in the time difference of such aging phenomena according to the stress levels (e.g. over-aging at the low stress level) and then resulting in the decrease of the fatigue strength and life factor.

Consequently, it seems that the fatigue life factor could be increased by proper aging treatment, resulting in increasing the

fatigue life for the friction welded joint as well as the base metals.

### 3-4. Microscopical Examination for Fatigue Crack Behavior at Welded Zone

Figure 5 shows the typical microstructures of the rotary bending fatigue fractured surfaces for the friction welded joints SUH 3-SUS303 at the room temperature (Specimen W) and the elevated temperature of 700°C (Specimens W<sub>T</sub>, W<sub>T0A</sub>, W<sub>T10A</sub>, W<sub>T100A</sub> as non-heat treated or postweld-heat treated as shown in Table 5). All the fractured shapes were almost similar and the fractures occurred at the base metal SUS303 side, but, in the case of the non-heat treated joint (W) at the room temperature test, the fracture took place at the heat affected zone of SUS303 side.

As SUS303 was added with much amount of sulphur (S 0.296) for improving the machinability, so some elongated sulphide inclusions (MnS) re-oriented transgranularly along the interface could be microscopically observed at the interface vicinity area (between about 100 through 200μm far from the interface) of the base metal SUS 303 side of the welded joint as shown in Figure 5 (a). And so, it seems that cracks might be initiated or propagated from or along such sulphide inclusions but particularly more preferably from the chromium-carbide of (Cr, Fe)<sub>23</sub>C<sub>8</sub> precipitated finely at the austenite boundary and the inside-grain cleavage by the high temperature of about 500 through 800°C at the heat affected zone (but maximum over 1300°C<sup>15,16)</sup> at the interface) during friction welding and of 700°C on the whole surface during the elevated temperature rotary bending fatigue test.

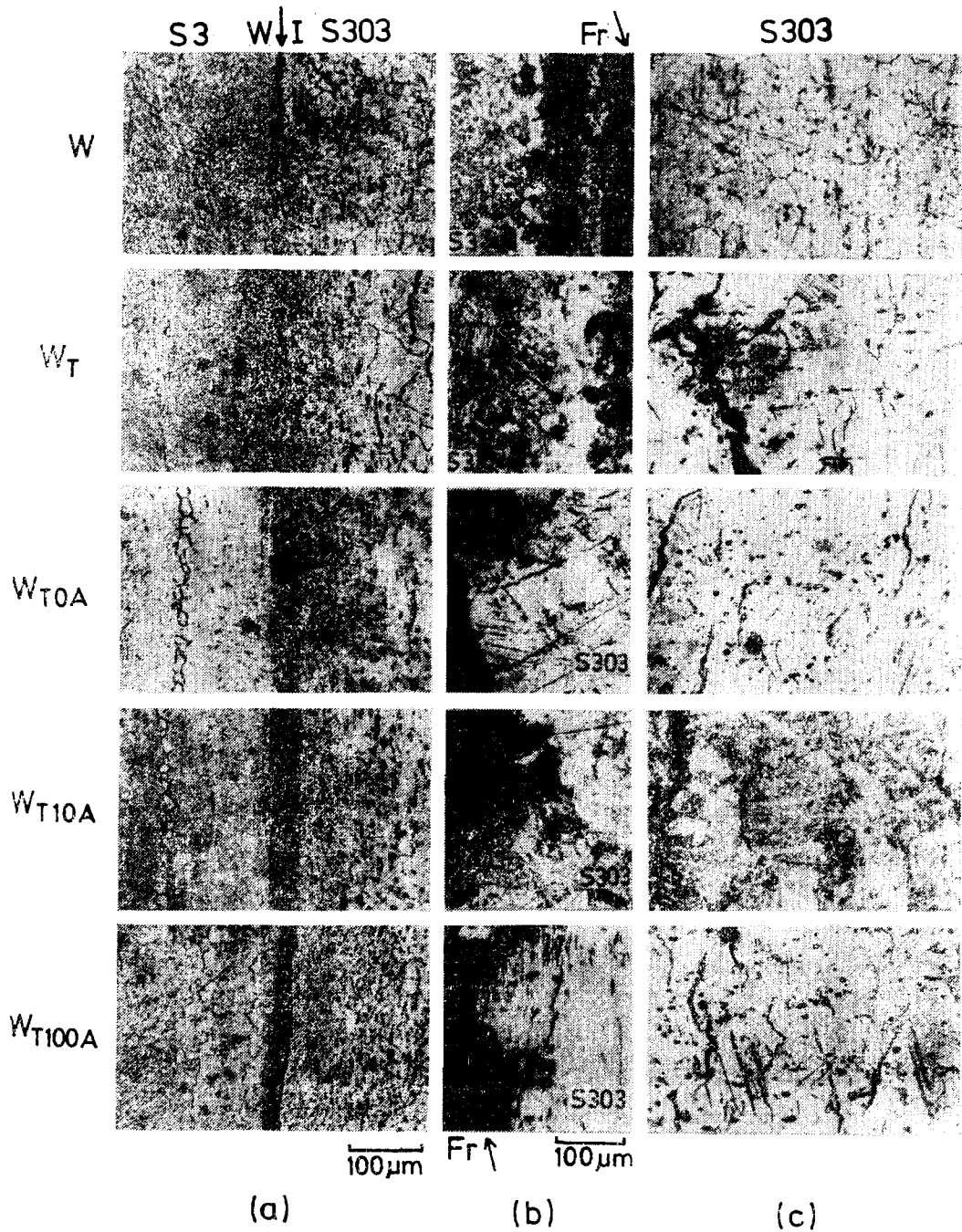


Fig. 5. Microstructures of the rotary bending fatigue fractured surfaces for friction welded joints SUH3-SUS303 (700°C):

(a) weld interface area,

(b) Fractured surfaces,

(c) Surface cracks at vicinity to the fractured position.

W-W<sub>T10A</sub>, W<sub>T100A</sub>, : Welded joints as in Table 5.

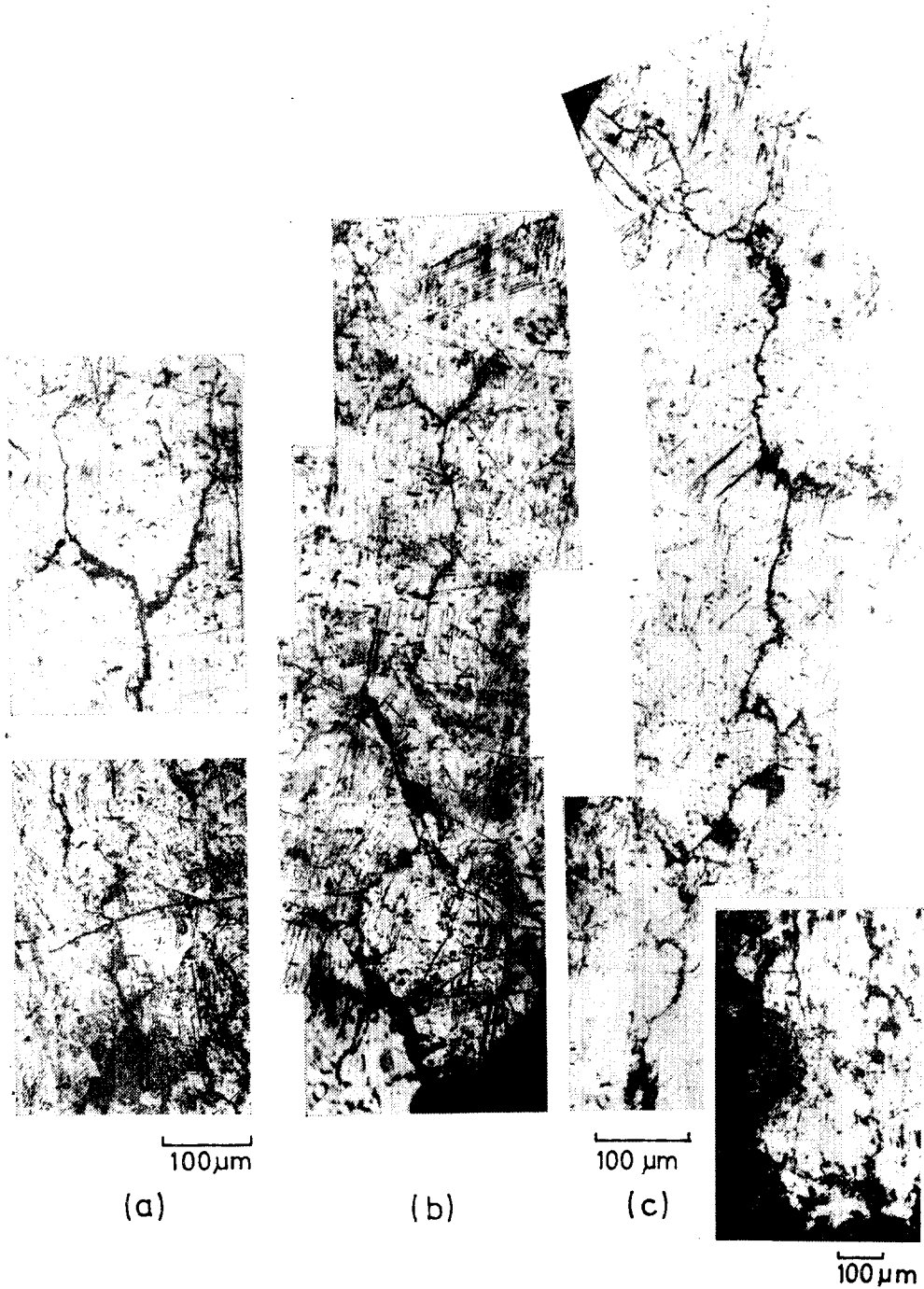


Fig. 6. Crack propagations on the rotary bending fatigue fractured surface of welded joint SUH3-SUS303:

- (a) Base metal S303;  $\sigma=30.19$ ,  $\sigma/\sigma_F=1.03$ ,  $N=1.06 \times 10^6$ ,
- (b) Welded joint W;  $\sigma=25.74$ ,  $\sigma/\sigma_F=1.07$ ,  $N=7.12 \times 10^4$ ,
- (c) Welded joint W;  $\sigma=25.05$ ,  $\sigma/\sigma_F=1.04$ ,  $N=6.67 \times 10^5$ .

And such cracks could be caused the most preferably from both combined sources (as shown in Figure 5 (b) and (c)— $W_T$ ,  $W_{T0A}$  and  $W_{T100A}$ ) or the inclusion pits (resulting in transgranular crack as shown in Figure 6 (a) and (c)) taken place mainly at the HAZ boundary of base metal SUS303 side. These kind of cracks could be interpreted as an intergranular corrosion<sup>17)</sup> of weld decay<sup>18)</sup> of austenitic stainless steel by corrosion fatigue<sup>17)</sup> under above-mentioned conditions and environment.

This is the reason why the fracture occurred at the base metal SUS303 side or its HAZ of the welded joint SUH3—SUS303 in the high temperature rotary bending fatigue test at 700°C as shown in Figure 5 (b) even though both hardness and strength of SUH3 at the elevated temperature of 700°C are lower than those of SUS303, expecting possibly that the fracture might occur at the SUH3 side just as the SUH3 side fracture in the case of the same high temperature (700°C) rotary bending fatigue test for the friction welded joint SUH3—SUH31 in the preceding report<sup>8,9)</sup>: Both SUH3 and SUH31 have no such weld decay but SUS303 does as shown in Figure 5 (a)— $W$  and (c).

Since such weld decay (intergranular corrosion) of SUS303 can be readily avoided by postweld annealing<sup>17)</sup>, the postweld aging heat treatment (precipitation hardening or age hardening)<sup>18)</sup> of 0, 10 and 100 h aging time at 700°C and air cooling, after the solution treatment (0 h aging) of 1060°C×1 h and water quenching, was taken as a feasibility test for precipitation hardening (PH) of the non-PH austenitic stainless steel SUS303 (Cr—Ni alloy) because the Cr—Ni austenitic heat resisting steel

SUH31 is known to be readily age-hardened<sup>19)</sup>. The experimental and analytic results were as remarkable as described in the preceding Sections 3-1 through 3-3. As shown in  $W_{T10A}$  of Figure 5 (a)—(c), almost no significant weld decay is observed in case of 10 h aging comparing with the other cases, resulting from the precipitation hardening effect. In the meantime, by the postweld-heat treatment such as solution treatment (0 hour aging in case of  $W_{T0A}$ ) and aging treatment (100 hour aging in case of  $W_{T100A}$ ), some amount of such cracks could be eliminated, as shown in  $W_{T0A}$  and  $W_{T100A}$  of Figure 5 (b) and (c). Avoiding such cracks by intergranular corrosion results in improving the high temperature fatigue strength as shown in Figure 2, Figure 3 and Figure 4.

Figure 6 (a) shows the typical intergranular crack propagation and the transgranular one of base metal SUS303 in room temperature rotary bending fatigue test, initiated at some inclusion pits of sulphide or non-metallic compound, and Figure 6 (b) and (c) show that the base metal SUS303 side of friction welded joint SUH3—SUS303 as non-postweld-heat treated has also very similarly such both types of cracks.

Consequently, it was microscopically confirmed that such characteristics of the high temperature fatigue strength improvement of welded joints is the most significant in the case of the 10 hour aging treatment by using the precipitation hardenability of the base metal austenitic stainless steel of the welded joint.

### 3-5. Experimental Consideration on Improvement of High Temperature Fatigue Strength of Friction Welded Joints by Aging Treatment

A consideration was taken on improving the high temperature (700°C) rotary bending fatigue strength of the friction welded joints (SUH3-SUS303) by postweld aging treatment after solution treatment through experiments and quantitative analysis.

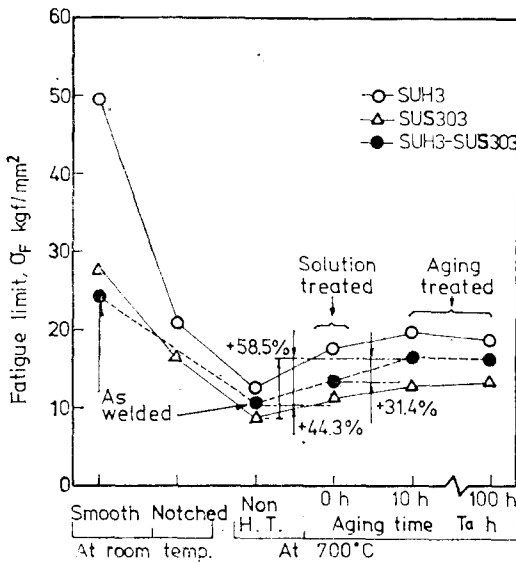


Fig. 7. Effects of aging treatment on fatigue limit. Welding and heat treatment conditions; as in Table 3 and 4.

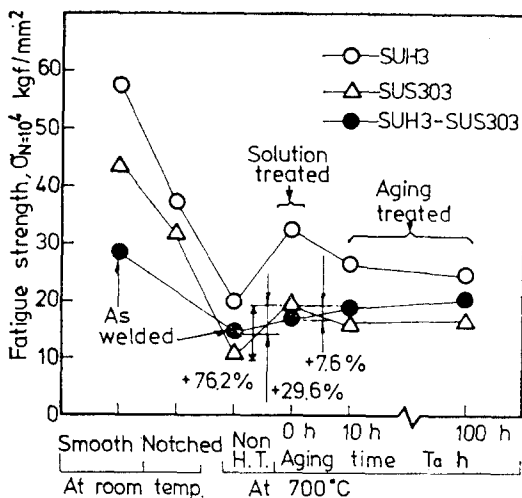


Fig. 8. Effects of aging treatment on fatigue strength ( $N=1 \times 10^4$ ). Welding and heat treatment conditions; as in Table 3 and 4.

Figure 7 and Figure 8 show the effects of aging treatment on the rotary bending fatigue limits and fatigue strengths, respectively, by the empirical Equations (2) through (18): One of the remarkable results represents that the high temperature (700°C) fatigue limit and fatigue strength ( $N=10^4$ ) of friction welded joint SUH3-SUS303 as 10 h aging treated at 700°C after postweld solution treatment of  $1060^\circ\text{C} \times 1 \text{ h}$  & water cooling was improved to 44.3% and 29.6% increase more than those of the welded joint as welded (non-heat treated) and 31.4% and 7.6% increase more than those of the joint as solution treated while 58.5% and 76.2% increase, respectively, more than those of the base metal SUS303 as non-heat treated, at which the fatigue fracture occurred.

#### 4. Conclusions

The obtained results from the experimental and analytical study on improvement of high temperature fatigue strength of the friction welded joints SUH3-SUS303 by postweld aging treatment after solution treatment are as follows:

(1) By aging treatment ( $700^\circ\text{C} \times 10 \text{ h}$ , A. C. after solution treatment of  $1060^\circ\text{C} \times 1 \text{ h}$ , W. C.), the high temperature (700°C) rotary bending fatigue limit of the friction welded joints (SUH3-SUS303) were increased to about 44.3% more (about 58.5% more than that of base metal SUS303) than those of as-welded and non-heat treated joints, and the high temperature fatigue strength ( $N=10^4$ ) at 700°C to about 29.6% more (about 76.2% more than that of base metal SUS303).

(2) It seems that the fatigue life factor could be increased by such aging treatment, resulting in lengthening the fatigue life for the friction welded joint as well as the base

metals.

(3) It was found that the empirical fatigue limits were very equivalent (about 7.5% lower) to the calculated ones by Pantereb's formula. The obtained empirical equation model is very reliably expressed as

$$\log N = -(a \sigma_B + b)^{0.5} + c.$$

(4) It was microscopically confirmed that the characteristics of the high temperature fatigue strength improvement of welded joints is the most significant in the case of the 10 hour aging treatment.

(5) It was also found by micro-examination that the 10 h aging after solution treatment produced more significant and proper precipitation hardening effect than any others, avoiding the weld decay problems of austenitic stainless steel SUS303 and resulting in improving the high temperature fatigue strength of the welded joint.

## References

- 1) Kuwahara, K., A. Nitta, "On High Temperature Fatigue and Creep Strength of a 2 Cr-1 Mo Steel Pipe Material Used for a Long Period," Cent. Res. Inst. of El. Pow. Ind. (CRIEPI) Report E279002, 1972, p. 1-45.
- 2) Murakami, K., M. Ikeuchi, A. Nishioka, W. Kawahara, "Aging Properties of Two-Phase ( $\alpha$ - $\gamma$ ) Stainless Steel Weldment," J. JWS, Vol. 49, No. 3, 1980, p. 213.
- 3) Shioya, T., S. Yamada, Y. Kuzuya, "Study on Welding Conditions for Steel by Friction Welding," J. JWS, Vol. 34, No. 8, 1965, p. 794
- 4) Um, D. S., S. K. Kang, "Study on Fatigue Strength of Friction Welded S20C and SUS-27B," J. SNAK, Vol. 8, No. 2, 1971, p. 13.
- 5) Moore, T. J., "Welding Journal, J. AWS, Vol. 51, No. 4, 1972, p. 253.
- 6) Oh, S. K., "Studies on Strength Analysis of Friction Welded Joints and In-Process Monitoring of the Welding Using Acoustic Emission Techniques," Ph. D. Dissertation, Keio University, Japan, 1982, p. 85-146, p. 305-314.
- 7) Pantereb, B. M., "Fracture of Metals (V. S. Ivanova)," Trans. by T. Yokobori, 1970, p. 190.
- 8) Oh, S. K., K. Y. Lee, H. J. Kim, "A Study on Fatigue Strength of Friction-Welded Heat-Resisting Steels at High Temperature (1)," Proc. KSME, June, 1980, p. 130-138.
- 9) Oh, S. K., K. Y. Lee, "Studies on Friction Welding and Welded Joint's Fatigue Strength of Heat Resisting Dissimilar Steels Used for Aeroplane or Marine Engine Components, Bull. N. F. U. of Busan, Vol. 20, No. 2, 1980, p. 49-87.
- 10) Weibull, W., "Statistical Representation of Fatigue Failure in Solids, Acta Polytechnical Stockholm, 1949.
- 11) Sors, L., "Fatigue Design of Machine Components, 1971, p. 6.
- 12) Stüssi, "Fatigue Design of Machine Components by L. Sors," 1971, p. 6.
- 13) JSME, "Data on Fatigue Design of Metals," JSME, 1977, p. 147.
- 14) Japan Steel Ass., "Heat Treatment of Steels," JSA, 1970, p. 560.
- 15) Wang, K. K., P. Nagappan, "Transient Temperature Distribution in Inertia Welding of Steels," AWS Welding Research Supplement, Sep., 1970, p. 424, 425.
- 16) Hasui, A., "Friction Welding," JFWRC, Corona Pub. Co., 1979, p. 35.
- 17) AWS, "Welding Handbook," AWS, Vol. 3, 1980, p. 203.
- 18) Hasui, A., "Friction Welding," JFWRC, Corona Pub. Co., 1979, p. 50, 200.
- 19) AWS, "Welding Handbook," AWS, Vol. 3, 1980, p. 113-117, 121, 133.